Dist. Category UC-90C

MATERIALS RESEARCH FOR CLEAN UTILIZATION OF COAL

QUARTERLY PROGRESS REPORT

January 1 - March 31, 1978

Samuel J. Schneider
Project Manager

Center for Materials Science
National Bureau of Standards
Washington, D. C. 20234

PREPARED FOR THE UNITED STATES
DEPARTMENT OF ENERGY

Under Contract No. EA-77-A-01-6010

EA-6010-15
Dist. Category UC-90C

MATERIALS RESEARCH FOR CLEAN UTILIZATION OF COAL

QUARTERLY PROGRESS REPORT

January 1 - March 31, 1978

Samuel J. Schneider
Project Manager

Center for Materials Science
National Bureau of Standards
Washington, D. C. 20234

PREPARED FOR THE UNITED STATES
DEPARTMENT OF ENERGY

Under Contract No. EA-77-A-01-6010

TABLE OF CONTENTS

I. OBJECTIVE AND SCOPE OF WORK

Coal Gasification processes require the handling and containment of corrosive gases and liquids at high temperature and pressures, and also the handling of flowing coal particles in this environment. These severe environments cause materials failures which inhibit successful and long-time operation of the gasification systems. The project entails investigations on the wear, corrosion, chemical degradation, fracture, and deformation processes which lead to the breakdown of metals and ceramics currently being utilized in pilot plants. Studies will also be carried out on new candidate materials considered for improved performance. Special emphasis will be devoted to the development of test methods, especially short-time procedures, to evaluate the durability of materials in the gasification environments. These methods will focus on wear, impact erosion, stress corrosion, strength, deformation, slow crack growth and chemical degradation. A system has been initiated to abstract and compile all significant operating incidents from coal conversion plants as well as materials property and performance information important to the design and operation of these plants. This program will provide a central information center where problems of common interest can be identified and analyzed to avoid unnecessary failures and lead to the selection of improved materials for coal conversion and utilization. Active consultation to DoE and associated contractors will be provided as requested.

II. SUMMARY OF PROGRESS TO DATE

Brief Summary

1. Metal Corrosion

a. Slow Strain Rate Test

A thorough metallographic examination of the alloy specimens tested in helium, oxidizing/sulfidizing gas mixture, and oxidizing/sulfidizing/carburizing gas mixture at 450 °C (840 °F), and 600 °C (1100 °F) at a strain rate of 10^{-6}/s was completed. Of the six alloys tested, four (Types 310 SS, 310S SS, nickel alloy 800, and nickel alloy 671) were found to be susceptible to cracking at 600 °C by possibly different mechanisms, however, all were detected by the slow strain rate technique. A summary report is in progress of all the progress to date of the slow strain rate testing technique. A preliminary evaluation was done on wedge-loaded DCB* specimens that were received from the Synthane plant. These specimens were exposed in the liquid phase of the scrubber surge tank. The preliminary evaluation showed that little, if any, cracking occurred in any of the specimens during the exposure at 196 °C (385 °F). Some design changes were made to the pulse echo ultrasonic equipment to be purchased by NBS for *in situ* monitoring of the cracking progress of specimens while they are being tested.

*Double cantilever beam.

A follow-up summary report will be submitted. We will complete the evaluation of the DCB specimens exposed in the Synthane plant; install NBS purchased resistivity equipment for *in situ* monitoring of the cracking progress of specimens while they are being tested.

b. Pre-Cracked Fracture Test

A temperature compensated DCB test specimen has been developed for conducting stress-corrosion tests *in situ* at elevated temperatures. This specimen is independent of temperature. For example, a specimen of 310 stainless steel would show a change of less than 4% in the stress intensity on heating from room temperature to 700 °C.

2. Ceramic Deformation, Fracture and Erosion

A high-alumina (94%) refractory concrete was exposed to a simulated coal gasification environment of gaseous H_2O, CO, CO_2, H_2 and CH_4 at temperatures of 510°, 710°, and 910 °C, and at a pressure of 7.5 MPa (~1090 psi). Room temperature flextural strength did not seem to be affected by exposu under these test conditions. In addition, the hot strength of a low-alumi refractory concrete was measured both before and after hydrothermal treatment. An improvement in the hot strength on hydrothermal treatment was obtained throughout the useful temperature range of the refractory. The construction and assembly of the high temperature, high-pressure mechanica loader has entered its final phase. All valving necessary for the operati of a pressure balancing unit which will regulate the pressure between the inner containment vessel and the outer pressure vessel has been completed.

3. Chemical Degradation

a. Reactions and Transformations

Energy dispersive powder diffraction patterns obtained in two series of experiments with high alumina neat cement bars heated in steam have been interpreted by visual inspection using the reference patterns prepared earlier. Computer methods developed during the past quarter to assist in the interpretation have also been applied. During the next quarter, the studies will be extended to include a lime-alumina-silica refractory in steam and in a complex simulated gasification environment.

b. Slag Characterization

The high pressure viscometer is currently operational and preliminary viscosity measurements have been made up to 95 psi steam pressure (at 1100 °C).

c. Vaporization and Chemical Transport

A new type of capillary sampling probe, suitable for corrosive slag atmospheres, has been developed and tested on an alkali silicate system where significant vapor transport of sodium-containing species was found. Conditions whereby thermodynamic equilibrium is approached in our reactor and with minimal perturbation by the sampling process have been established for a conical probe. Thermodynamic equilibrium modeling of vapor transport in slag-coal gas systems was initiated and sodium vapor transport demonstrated theoretically.

The new sampling probe will be characterized for its ability to sample equilibrium systems without perturbation. More detailed experimental and modeling studies of slag-coal gas vapor transport will be carried out.

4. Failure Prevention

a. Failure Information Data Center

Thirty-seven additional reports of operating experiences and failure analysis were entered into the Center's data base. A detailed analysis of the performance of materials and components at the CO_2 Acceptor Process Plant was completed and a report is in preparation. Additional progress was made on a similar report covering the Hygas Pilot Plant.

b. Materials Properties Data Center

The work of the Center has continued with the handling and cataloguing of reports, the initiation of a thesaurus which will be needed at a later stage for computer file cataloguing and searching, further study and planning for a suitable Data Base Management System, drawing up of final specifications for the equipment for the computer-terminal facility, the ordering of the first four pieces of equipment to establish the facility, and the preparation and revision of summary report.

Articles Published and Talks Presented

J. H. Smith, "Operating Experiences with Incoloy 800 in Coal Conversion Process Plants," a talk presented at the Petten International Conference - Alloy 800, Petten (N. H.), The Netherlands, March 1978.

G. M. Ugiansky and C. Johnson, "Slow Strain Rate Stress Corrosion Testing of Metals in Gaseous Atmospheres at Elevated Temperatures," planned (article under review) for publication in the Proceedings of ASTM Sympsoium: Stress Corrosion Cracking--The Slow Strain Rate Technique, May 2-4, 1977, Toronto, Canada.

S. M. Wiederhorn, "Erosion of Castable Refractories," Fourteenth Annual Symposium on Refractories, sponsored by the American Ceramic Society, St. Louis, Missouri, April 7, 1978.

III. DETAILED DESCRIPTION OF TECHNICAL PROGRESS

1. Metal Corrosion

a. Slow Strain Rate Test (G. M. Ugiansky and C. E. Johnson, 561)

Progress: A detailed report is being prepared on the Slow Strain Rate Test for submission as a special report. The abstract of that report is as follows:

A total of six different alloys -- stainless steel (SS) Types 310, 310S, 347, and 446, and nickel alloys 800 and 671 -- were tested using the slow strain rate test technique in oxidizing/sulfidizing and in oxidizing/sufidizing/carburizing simulated coal gasification environments, and in helium (and other inert environments) at both 450° and 600 °C at a strain rate of 10^{-6}/s. Of the six alloys, four (Types 310 SS, 310S SS, nickel alloy 800, and nickel alloy 671) were found to be susceptible to cracking at 600 °C by possibly different mechanisms, however, all were detected by the slow strain rate technique.

For cracking, the nickel alloy 671 required no reactive environment -- it suffered internal cracking in helium and all other test environments used. However, the stainless steel Types 310, 310S, and nickel alloy 800, all of which failed through surface initiated cracking, required increasingly severe environments for cracking. The Type 310 SS required very little reactive environment -- it cracked not only in the simulated coal gasification gases but also in low vapor pressure O_2 and/or H_2O environments (for example, helium), as did the 310S SS, although with greater ductility than the Type 310 SS. The nickel alloy 800 required the rather reactive environment of the simulated coal gasification gases -- it did not crack in the low vapor pressure O_2 and/or H_2O environments.

The detection of the environmentally independent failure of alloy 671 shows that the use of the slow strain rate technique need not be limited to use for testing for susceptibility to cracking by stress corrosion cracking. The slow strain rate technique is shown to be a viable testing method for detecting an alloy's propensity to premature failure in gaseous simulated coal gasification environments.

During this quarter, the testing of stainless steel alloys Types 310, 310S, 347, 446, and nickel alloys 800 and 671 has been completed in the oxidizing/sulfidizing (previously called oxidizing) and in the oxidizing/sulfidizing/carburizing (previously called reducing) coal gasification environments and in an inert gas environment (ultra-pure He) at 450 °C and 600 °C at a strain rate of 10^{-6}/s. The compositions of the simulated coal gasification gases are shown in Table 1. The major difference between the two mixtures is the deposition of carbon from the oxidizing/sulfidizing carburizing gas at both temperatures, the oxidizing and sulfidizing potential being similar when comparing the two mixtures at the same temperature.

Metallographic examinations of the tested alloy specimens have been completed and a thorough summary report (soon to follow) of all results and their significance is currently being prepared. In brief, the results show that of the six alloys tested, at 600 °C four (Type 310 SS, Type 310S SS, and nickel alloys 800 and 671) were found to be susceptible to intergranular cracking. Two of the alloys (Type 310 SS and nickel alloy 671) failed with relatively low ductility compared to the other two alloys (Type 310 S SS and nickel alloy 800) when tested at 600 °C. None of the alloys cracked when tested at 450 °C in either of the coal gasification environments or in He. In earlier tests, it was noted that Type 310S SS did not show any susceptibility to cracking when tested at 540 °C, but the increase in temperature to 600 °C resulted in cracking of the Type 310S SS. The Type 310S SS, with the lower carbon content than Type 310 SS, has to be subjected to a higher temperature or a longer time at temperature for sensitization and, therefore, cracking to occur. The alloy compositions can be found in Table 2. The reported cracking failures were possibly due to different mechanisms, however, all were detected by the slow strain rate technique. The specific environmental conditions needed for cracking of the above mentioned four alloys are summarized in Table 3. The detection of the failure of nickel alloy 671 by an internal cracking mechanism shows that the use of the slow strain rate technique need not be limited to use for testing for susceptibility to cracking by stress corrosion cracking (SCC).

Some of our wedge-loaded DCB specimens exposed in the Synthane plant have been received. These specimens were from the liquid phase scrubber surge tank with the liquid effluent summarized in Table 4. The specimens were Types 304 SS, 309 SS, 310 SS, 446 SS, nickel alloy 800, nickel alloy 671, and low carbon steel AISI 1018-20. The specimens were exposed for a combined time of 2046 hours (592 hours operating time and 1454 hours standby time) at an average operating temperature of 196 °C (835 °F) and a pressure of 600 psig. The as-received exposure rack is shown in Fig. 1. One of the exposed specimens is shown in Fig. 2. Preliminary evaluation of the specimens (i.e., measurement of the crack growth without splitting apart of the specimen) shows that little, if any, crack growth occurred during testing on any of the specimens. After the exposure, the specimens were coated and pre-cracked areas were packed full with a solid deposit (Fig. 2). Further evaluation of these specimens by splitting them apart and measuring the crack length will be done.

Some design changes are being made in the pulse echo ultrasonic equipment to be purchased by NBS for *in situ* monitoring of the cracking progress of specimens while they are being tested.

Plans: Submit follow-up summary report. Finish evaluation of the DCB specimens exposed in the Synthane plant. Install NBS purchased resistivity equipment for *in situ* monitoring of the cracking progress of specimens while they are being tested.

TABLE 1 GAS COMPOSITIONS[1]

(Vol. %)

	Oxidizing/Sulfidizing Gas[2]			Oxidizing/Sulfidizing/Carburizi		
	INPUT	EQUILIBRIUM		INPUT	EQUILIBRIU	
	1atm, 25°C	1atm, 450°C	1atm, 600°C	1atm, 25°C	1atm, 450°C	1at
CO	11.6	1.2	9.2	26.0	1.1	
CO_2	15.4	24.9	20.6	14.8	22.0	
H_2	13.0	16.0	36.3	26.0	12.8	
CH_4	10.0	12.5	2.9	10.0	11.2	
H_2S	1.0	1.0	0.9	1.0	1.0	
H_2O	49.0	44.4	30.3	22.2	34.3	
C	-	-	-	-	17.6	
log P_{O_2}		-28.995	-23.919		-29.026	
log P_{S_2}		-10.260	-8.878		-10.086	
log a_c		-0.043	-0.288		+0.017	

Footnotes:

(1) The gas mixtures are two of twelve mixtures being used at Battelle Columbus Laboratories and Argonne National Laboratory.

(2) This mixture corresponds to Battelle's "Gas Mixture 1A." [7]

(3) This mixture corresponds to Battelle's "Gas Mixture 3A." [7]

Note: The major difference between the two mixtures is the deposition of carbon from the oxidizing/sulfidizing/carburizing gas at both temperatures, the oxidizing and sulfidizing potentials being similar at each temperature.

Table 2

Alloy Compositions, Weight %*

Alloy	C	Mn	Si	S	P	Nb	Ta	Ti	Cu	Mo	Ni	Cr	Fe	Heat Treatment
Type 310 SS	0.08	1.78	0.48	0.02	0.028				0.17	0.10	19.59	21.84	Bal	Cold drawn, Annealed 1010-1150 C, water quench, pickled (HNO_3 - HF)
Type 310S SS	0.06	1.68	0.72	0.011	0.017				0.14	0.11	19.60	24.67	Bal	Same as 310 SS
Type 347 SS	0.06	1.45	0.69	0.01	0.024	.64	.02		0.28	0.43	9.49	18.21	Bal	Cold drawn, Annealed 980-1090 C, water quench, pickled (HNO_3 - HF)
Type 416 SS	0.11	0.52	0.47	<0.005	0.035				0.03	0.13	0.59	25.77	Bal	Cold drawn, Annealed 790-870°C, water quench, pickled (HNO_3 - HF)
Nickel alloy 800	0.01	0.93	0.29	0.01	0.005			0.38	0.54	0.03	32.51	20.02	Bal	Cold drawn, Solution annealed 980-1040°C, pickled
Nickel alloy 671	0.06							0.30			50.27	46.74		Cold drawn, Solution annealed 1150°C, Pickled

(*) From quantitative analyses

Table 3

Alloys and Conditions for Cracking

Alloy:	Nickel alloy 671	310 SS - 310S SS	Nickel alloy 800
Environment needed for Cracking at 600°C:	No reactive environment needed. Internal cracking in He and all other environments.	Minimal reactive environment needed. Surface cracking in coal gasification gases and in low vapor pressure O_2 and/or H_2O environment (e.g., He)	Reactive environment needed. Surface cracking in coal gasification gases but not in low vapor pressure O_2 and/or H_2O environment (e.g., He)

Table 4

Liquid Effluent from Scrubber
Surge Tank

Phenols (ppm)	0-12,500
Chemical Oxygen Demand (ppm)	100-71100
p-Alkalinity (gms/gal)	0-77
m-Alkalinity (gms/gal)	0-743
N as NH_3 (ppm)	0-4410
S (ppm)	5-346
Chlorine (ppm)	95-153
Dissolved Solids (ppm)	50-2100
Thiocyanate (ppm)	No Data
Cyanide (ppm)	No Data
pH	5.2-9.5
Total Suspended Solids (weight %)	0-67

Fig. 1. Wedge-loaded DCB specimen exposure rack from the liquid phase of the scrubber surge tank from the Synthane plant.

Fig. 2. Wedge-loaded DCB specimen from the liquid phase of the scrubber surge tank after 2046 hours at an average temperature of 196°C (385°F).

b. Pre-Cracked Fracture Test (J. H. Smith, 562.00)

Progress: A tension-loaded, double cantilever beam specimen has been designed for conducting elevated temperature stress-corrosion tests. This specimen is a modification of the wedge-loaded double cantilever beam specimen which is extensively used for stress corrosion testing at ambient temperature.[1] The susceptibility to stress-corrosion cracking is expressed in terms of the stress intensity factor, K_I. The crack growth rate, da/dt, due to stress-corrosion cracking is proportional to the stress-intensity, K_I, and the minimum stress-intensity value below which crack propagation is not observed is designated as K_{ISCC}. Both the commonly used wedge-loaded double cantilever beam specimen and the newly designed tension-loaded double cantilever beam specimen have the advantage, for stress-corrosion testing, that the applied stress-intensity, K_I, decreases as crack growth occurs so that in principle, the minimum stress-intensity value below which crack growth will occur, that is K_{ISCC}, can be determined with a single test specimen.

If the dimensions of the double cantilever beam specimen, Figure 1, are chosen such that the length of the specimen $W \geq a + 2H$, where 'a' is the crack length and 2H is the specimen height, the stress intensity, K_I, calibration for the specimen is independent of the uncracked ligament in the specimen, (W-a), and the stress intensity for the specimen is:[1]

$$K_I = \frac{Pa}{BH^{3/2}} \left[3.46 + 2.38 \frac{H}{a}\right]$$

where:

P - applied load
a - crack length
B - specimen thickness
H - specimen height

For a specimen that is loaded by displacement control instead of load control, the load, P, is related to the displacement, V, at the loading point by the relationship:

$$P = \frac{EBV}{7.97 \left(\frac{a}{H}\right)^3 + 16.48 \left(\frac{a}{H}\right)^2 + 11.32 \left(\frac{a}{H}\right)}$$

where E is the elastic modulus of the specimen.

By combining equations [1] and [2] the stress intensity is given in terms of the displacement as:

$$K_I = \frac{EV}{H} \left[\frac{3.46 + 2.38 \left(\frac{H}{a}\right)}{7.97 \left(\frac{a}{H}\right)^2 + 16.48 \left(\frac{a}{H}\right) + 11.32}\right]$$

This equation is applicable to a double cantilever beam specimen loaded to a specified displacement, V, under the following conditions:

$$W = a + 2H$$

$$2 \leq \frac{a}{H} \leq 10$$

$$a \geq 2.5 \left(\frac{K_I}{\sigma y}\right)^2$$

where σy is the yield strength of the specimen material.

Equation (3) is used as the basis for designing a double cantilever beam specimen that can be loaded to a specified K_I level at room temperature and used for testing at elevated temperature without a substantial change in the initial applied stress intensity level, K_I, due to the change in temperature. Once crack growth starts due to stress corrosion cracking at the elevated temperature, the stress intensity decreases with crack growth until the K_{ISCC} level is reached according to equation (3).

The tension-loaded double cantilever beam specimen, shown in Figure 2, was designed to be independent of testing temperature. Equation (3) shows that the stress intensity, K_I, is directly proportional to the elastic modulus of the test specimen, E, and the applied displacement, V, and to a function of the crack length, a, to specimen height, H, ratio, a/H. Only the elastic modulus, E, and the applied displacement, V, change significantly with temperature. Therefore, the ratio of the stress intensity at a specified temperature, K_T, to the stress intensity at a reference temperature, such as room temperature, K_o is given as:

$$\frac{K_T}{K_0} = \frac{E_T V_T}{E_0 V_0},$$

where E_T and V_T are the elastic modulus and applied displacement at the specified temperature, T, and E_0 and V_0 are the modulus and displacement at the reference temperature, T_o.

The tension-loaded double cantilever beam specimen, Figure 2, is designed so that thermal expansion of the loading fixture on increasing temperature will nearly balance the decrease in elastic modulus with increasing temperature so that the ratio

$$\frac{K_T}{K_0} = 1.0.$$

That is, $\frac{K_{IT}}{K_{IO}} = \frac{E_T V_T}{E_0 V_0} = 1.0$

The change in elastic modulus, E with temperature has been determined for all common alloys. In general, the modulus of elasticity of common alloys decreases approximately linearly with temperature up to relatively high temperatures beyond which a sharp drop in modulus occurs. For example, austenitic stainless steels and Ni-Cr-Fe alloys such as Incoloys show a linear decrease in modulus with increasing temperature up to approximately 1300°F (704°C).[2] Therefore, the change in elastic modulus with temperature can be expressed as: $E_T = E_0 - m\ (T - T_0)$ where m is an empirically determined coefficient. For example, up to 700°C (1300°F) stainless steel alloys follow the relationship $E_T = E_0 - 11.0 \times 10^3\ (T - T_0)$ where E is in units of psi and T is °C.[2]

The applied displacement, V, at the loading point of the DCB specimen can be made to either increase or decrease as the temperature increases. The initial displacement, V_0, is applied mechanically on loading the specimen at room temperature. The displacement, V_T, at the elevated temperature, T, is controlled by the difference in thermal expansion between the specimen and loading fixtures. The change in stress-intensity with increase in temperature is given by the following expression:

$$\frac{K_T}{K_0} = \{1 - \frac{mT}{E_0}\}\ \{1 + \frac{(\ell_{T,F} - \ell_{T,S} - \ell_{T,G})}{V_o}\}$$

where:

K_T - stress-intensity of the specimen at test temperature, T.

K_0 - stress-intensity of the specimen at reference (loading) temperature.

m - temperature coefficient of the elastic modulus of the specimen.

E_0 - elastic modulus of the specimen at reference temperature T_0.

T - test temperature of interest.

V_0 - initial displacement of the specimen at temperature T_0.

$\ell_{T,F}$ - length of loading frame at temperature T (see Figure 2)

$\ell_{T,S}$ - length of specimen at temperature T.

$\ell_{T,G}$ - length of specimen grips at temperature T.

$\ell_{T,F} - \ell_{o,F}\ [1 + \alpha_F\ (T - T_0)]$

where $\ell_{o,F}$ is the length of the loading frame at temperature T_0 and α_F is the linear coefficient of thermal expansion from T_0 to T.

Similarly: $\ell_{T,S} = \ell_{0,S} [1 + \alpha_S (T - T_0)]$

$\ell_{T,G} = \ell_{0,G} [1 + \alpha_G (T - T_0)]$

for the specimen and loading grips, respectively.

In general the loading frame will be constructed of different material than either the specimen or the loading grips. By carefully choosing the combination of materials in the specimen, loading grips, and loading fixture, the specimen can be made temperature compensating, that is, $\frac{K_T}{K_0} = 1.0$ regardless of temperature. As the specimen is loaded to different initial displacements, V_0, the length of the loading grips, $\ell_{0,G}$, must be changed to permit K_T to be independent of temperature. This is the reason for the specimen loading fixture being designed as a form of "turnbuckle."

To demonstrate that the tension loaded double cantilever beam specimen can be made thermally compensating, a loading fixture made of 18-8 type stainless steel with a specimen of type 310 stainless steel and adjustable grips made of Monel was designed and analyzed. Figure 3 shows a plot of K_T/K_0 versus temperature up to 730°C (1350°F) for this specimen configuration. This shows that no decrease in K_T with temperature is expected up to approximately 550°C (1000°F) and that up to 730°C (1350°F) the decrease in K_I is only about 4% from the original "as-loaded" K level. By contrast, a wedge loaded double cantilever beam specimen cannot be made temperature compensating and the K_T level at 730°C (1350°F) would decrease to approximately 70% of the "as-loaded," room temperature value, as shown in Figure 3.

Ref.

1. B. F. Brown, "Stress-Corrosion Cracking in High Strength Steels, Titanium, and Aluminum," Naval Research Lab., 1972, Chap. 2.

2. F. Garofalo, P. R. Malonvek, G. V. Smith, "The Influence of Temperature on the Elastic Constants of Some Commercial Steels," ASTM, STP-129, 1952.

Plans: Plans for the next quarter are to:

1. Complete stress analysis for the tension-loaded double cantilever beam specimen. This is to include calculation of creep strains and a limited sensitivity analysis.

2. Calculation of $\frac{K_T}{K_0}$ versus temperature for various test materials of interest and various K_0 levle.s

3. Experimental verification of the $\frac{K_T}{K_0}$ equation by measurements of specimen compliance.

4. Procurement of selected alloys and specimen preparation for preliminary laboratory tests.

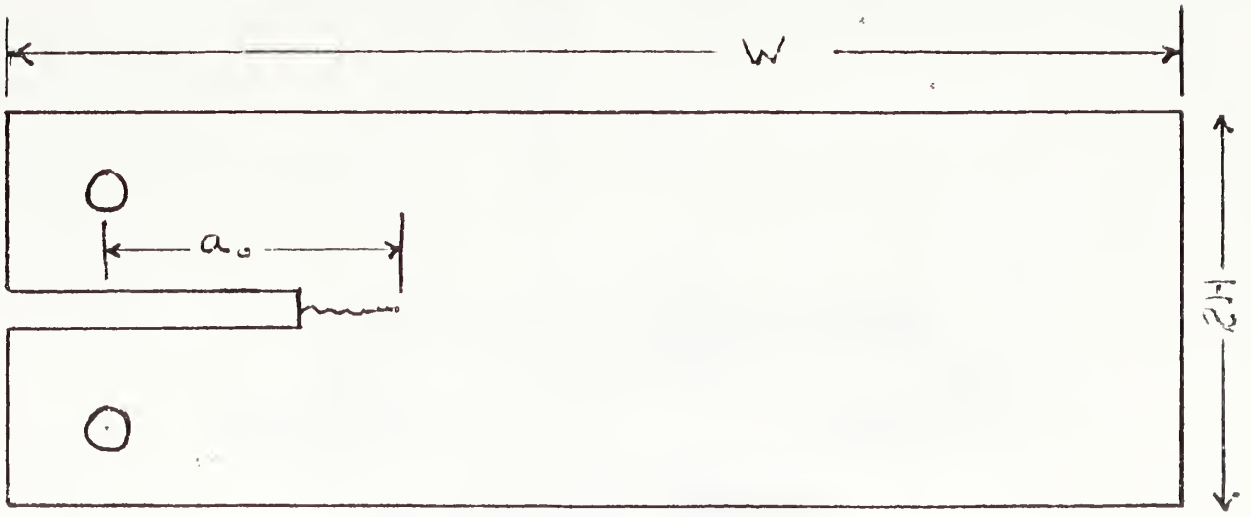

Design of Double-Cantilever
Beam Specimen

Figure 1

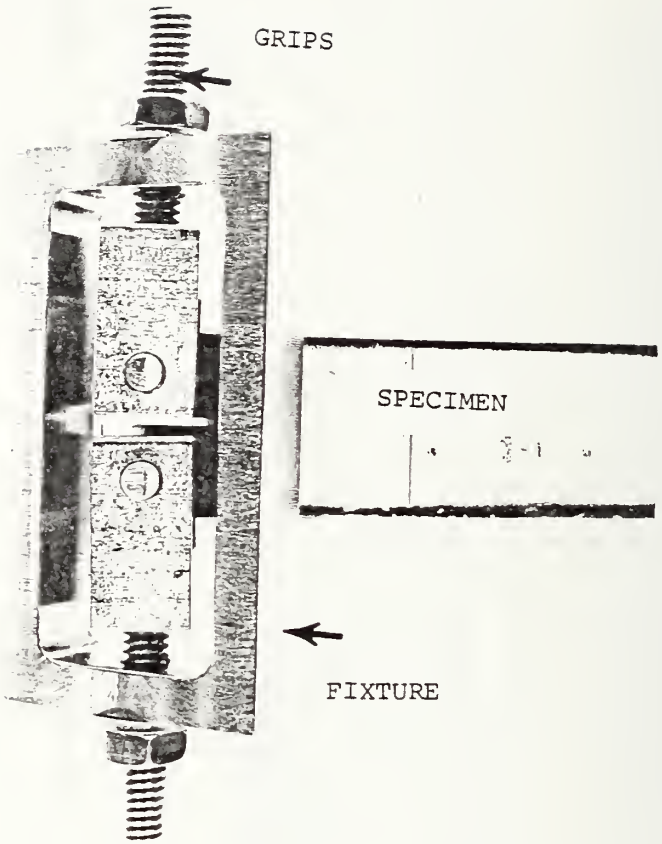

Figure 2

Tension - Loaded DCB Specimen

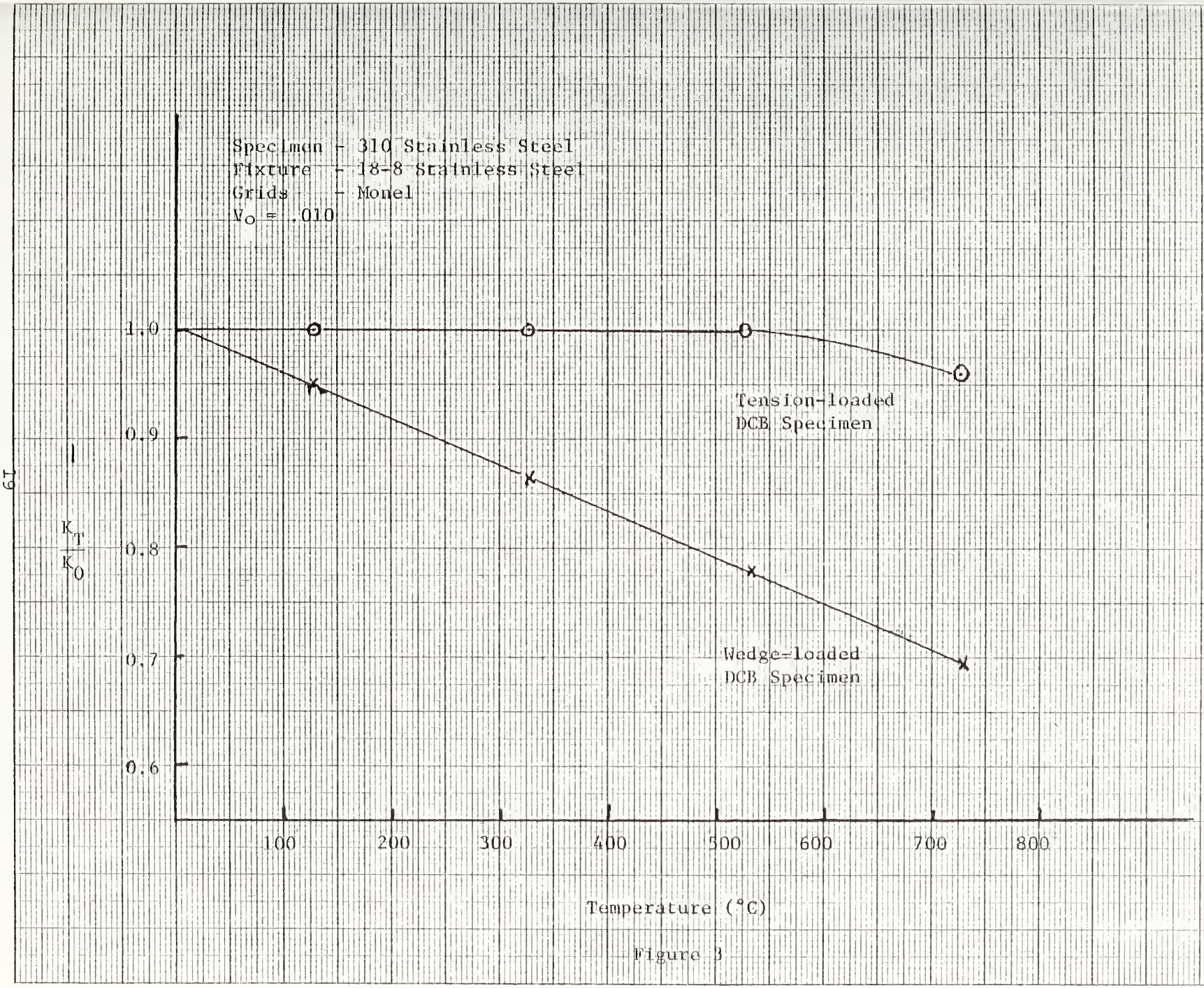
Specimen - 310 Stainless Steel
Fixture - 18-8 Stainless Steel
Grids - Monel
V_o = .010
1.0
0.9
0.8
0.7
0.6
$\frac{K_T}{K_0}$
Tension-loaded
DCB Specimen
Wedge-loaded
DCB Specimen
100
200
300
400
500
600
700
800
Temperature (°C)

Figure 3

2. Ceramic Deformation, Fracture, and Erosion (E. R. Fuller, Jr., S. M. Wiederhorn, J. M. Bukowski, and D. E. Roberts, 562, and C. R. Robbins, 565)

Progress: Exposure studies on a high-alumina (94%) refractory concrete in a simulated coal gasification environment were continued this past quarter. The ambient gas mixture for these studies was 40% H_2O, 20% CO, 15% CO_2, and 25% H_2 (Vol. %), which gives a gaseous environment of H_2O, CO, CO_2, H_2 and CH_4 at the temperature-pressure exposure condition. In this series of exposures, pre-fired* refractory concrete specimens were initially heated to the exposure temperature in an argon environment at atmospheric pressure. Once temperature equilibrium was reached, H_2O and a mixture of gaseous H_2, CO, and CO_2 were metered into the exposure vessel. Refractory samples were exposed to these simulated gasification environments at temperatures of 510°, 710°, 910 °C, and at a pressure of 7.5 MPa (∿1090 psi). After an exposure period of 90 hours, the specimens were allowed to cool to 500 °C at which point the exposure environment was slowly vented before cooling to room temperature. Room temperature flexural strength did not seem to be affected by exposure under these test conditions (Table 1). The determination of the mineralogical properties of the exposed high-alumina refractory concretes in progress.

Table 1

	TEMPERATURE			
	Control (Air-fired to 1010°C)	510°C	710°C	910°C
Flexural Strength**	14.8(±1.8) MPa	13.4(±2.4)MPa	16.1(±0.4)MPa	14.8(±1
	2,150(±260)psi	1,950(±340)psi	2,340(±60)psi	2,150(±

In addition to these exposure studies, the hot strength of a low-alumina (56%) refractory concrete has been measured both before and after hydrothermal treatment. Specimens treated hydrothermally were heated in a saturated H_2O environment to 310 °C and held for 65 hours at a pressure of 9.9 MPa (1430 psi). The temperature was then increased to 610 °C with the steam pressure being bled to maintain a constant 15.0 MPa (2180 psi). The refractory concrete specimens were held at temperature and pressure for 160 hours. On cool down, the steam pressure was slowly vented at

*1010 °C for 5 hours
**4 specimens tested at each condition

500 °C. The specimens were broken on a commercial testing machine using a constant cross-head speed of 5×10^{-3} cm/min. All specimens were heated at approximately 5 °C/min, and were allowed to soak at the test temperature for 15 hours before breaking.

Our previous studies on both a commercial composition and a laboratory-prepared composition of a low-alumina refractory concrete indicated that under certain conditions an increase in room temperature flexural strength and erosion resistance is obtained. The present studies examine this improvement in mechanical properties at elevated temperatures. The hot flexural strength of a hydrothermally exposed, low-alumina refractory was increased throughout the useful temperature range of the refractory (Figure 1). X-ray diffraction analysis indicates that the improved mechanical properties are related to the reaction of free silica, contained in the aggregate, with the calcium aluminate phases in the cement to form anorthite (CAS_2)*. The anorthite phase forms a strong, continuous structure of small crystallites that permeates and binds the refractory matrix. A determination of the hot erosive wear properties of this hydrothermally treated concrete is presently in progress. Since the room temperature erosion behavior after hydrothermal exposure seems to be controlled by the same microstructural properties that influence strength, an increase in the hot strength is also expected to increase the hot erosion resistance.

Compressive strength measurements were made on refractory concrete samples obtained from the CO_2 Acceptor Plant. In some cases, the low-alumina refractory concrete used at the hot face exhibited a compressive strength 2 to 3 times greater than air-fired laboratory specimens. X-ray diffraction analysis showed the presence of well crystallized anorthite to be present in the refractory samples obtained from the CO_2 Acceptor Plant. As in the hydrothermally treated refractory concretes, it is the formation of this anorthite that accounts for the increase in the compressive strength. A complete analysis of the examination will be published in a separate N.B.S. publication for the Department of Energy. In addition, a mineralogical and microstructural analysis is in progress for refractory concrete specimens exposed in the Synthane Process Pilot Plant.

The construction and assembly of the high-temperature, high pressure, mechanical loader has entered its final phase. All plumbing and valving necessary for operation of the pressure-balancing system of the mechanical loader has been completed. Presently, the electronic control system is being assembled and installed. This system is required to maintain a pressure equilibrium ($\Delta P=0$) between the inner containment vessel and outer pressure shell. On satisfactory installation and check out of the pressure balancing system, the mechanical loader will be operational, and systematic testing of refractory concretes will begin.

---

* Cement Chemistry Notation: C = CaO, S = SiO_2, H = H_2O, A = Al_2O_3

Plans: In the next quarter, assembly of the apparatus for mechanical testing at elevated temperatures and pressures should be completed. The total system will then be checked out under controlled experimental conditions. These experiments should establish the operation of the apparatus by the end of the quarter. Studies will then commence on refractory concretes under hydrothermal conditions.

Mechanical property studies at room temperature will continue on high and low-alumina refractory concretes after exposure to simulated coal gasification environments. After completion of the studies using a five component gasification environment (H_2O, CO, CO_2, H_2, and CH_4), more elementary studies will be conducted using two and three component gaseous systems such as H_2O, CO, and CO_2 and H_2O and H_2.

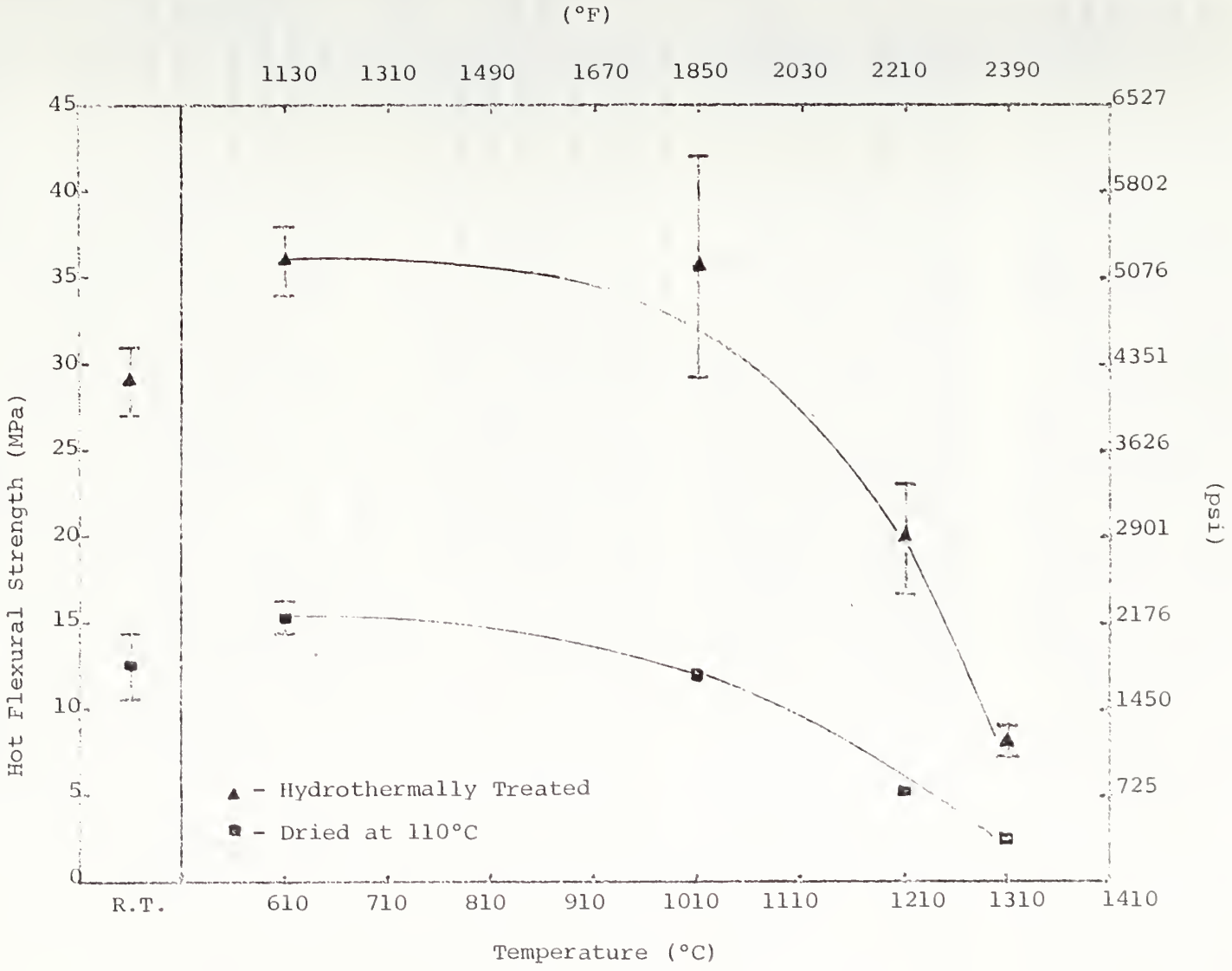

Figure 1. Hot flexural strength of a low-alumina (56%) refractory concrete before and after hydrothermal treatment.

3. Chemical Degradation of Ceramics

a. Reactions and Transformations (F. A. Mauer and C. R. Robbins, 565)

Progress: Two series of experiments using cast bars of high alumina neat cement have been carried out in a steam atmosphere. A third test of the neat cement in steam is underway. Although the primary purpose of the first two experiments was to test the performance of the apparatus, useful chemical information was obtained. All phase assemblages have been identified by visual inspection with the aid of the standard reference patterns prepared earlier and published in quarterly progress reports for Jan.-Mar. 1977 and Apr.-June 1977. Computer programs have also been prepared to assist in the analysis of patterns.

The first series of experiments was carried out using a bar of high alumina neat cement dried at 110°C and fired at 1010°C (specimen #2). This specimen, which consisted of CA_2* with small amounts of CA and α-Al_2O_3 was heated for 12 days in steam. The results are summarized in Table 1. Major changes are seen in the relative amoungs of CA_2 C_3AH_6, $C_4A_3H_3$, AH, and α-Al_2O_3. Although CA_2, C_3AH_6, and $C_4A_3H_3$ are usually considered to be the bonding phases of high alumina castable refractories, there is considerable interest in the role of AH because of earlier work by Fuller, Robbins, and Loeb[1] showing that the dissociation of this phase is associated with a dramatic loss in strength.

Table 1 shows that changes begin at temperatures as low as 93 °C. After 20 hours of exposure at 93°C, CA_2 was still the principal crystalline phase but the loss in intensity suggests that hydrates were forming which were not sufficiently well crystallized to give good diffraction patterns. As a result, C_3AH_6 and AH_3 appeared only as minor constituents. At 110°C after 46 additional hours of exposure only trace amounts of CA_2 remained. AH formed rapidly at 210°C but remained poorly crystalline after 4 hours. Crystallinity improved during the next 3 hours, and after 22 hours the test bar consisted of well crystallized C_3AH_6 and AH. After 15 hours at 365°C and 7.7 mPa,[2] $C_4A_3H_3$ and AH were the major phases with minor amounts of α-Al_2O_3.

The dissociation of the bonding phase, AH, and formation of α-Al_2O_3 was observed at 410°C and 7.9 mPa. This reaction proceeded slowly and AH was still a major phase after 24 hours. Even after 3 hours at 450°C and 7.9 mPa (a temperature that is approximately 100°C above its reported "equilibrium" region), AH was a major phase. Dissociation of the remaining AH occurred rapidly at 475°C and 7.9 mPa while CA_2 and CA began to form from $C_4A_3H_3$ and Al_2O_3. The amount of CA_2 increased during 16 hours

---

*Cement Chemistry Notation: C = CaO, S = SiO_2, H = H_2O, A = Al_2O_3.

[1] Quarterly Progress Report FE 1749-6, December 1975.

[2] In SI Units $p(mPa) = \frac{p(psig) + 14.7}{145}$

at 475°C and 3 hours at 500°C. Growth of the bonding phase, CA_2, at the expense of CA and α-Al_2O_3 proceeded slowly over the next 6 hours at 550°C and 575°C. At 600°C and 7.2 mPa the rate of formation of CA_2 appeared to increase significantly. The reaction was essentially completed after 18 hours. The phase assemblage CA_2 (major phase) and α-Al_2O_3 (minor phase) that resulted was observed at all temperatures and pressures up to 1000°C and 7 mPa. These observations suggest that, with the development of the CA_2 phase above 600°C, a high-alumina castable may regain some of the strength lost because of the dissociation of $C_4A_3H_3$ and AH.

The series of experiments with specimen #3 (high alumina neat cement dried at 110°C and fired at 1010°C) were carried out in steam over a 19 day period, and reached a maximum temperature of 995°C at 7 mPa. The results are of interest because the inadvertent use of a silica containing cement to secure the test bar in the pressure vessel subjected the specimen to an environment of SiO_2 dissolved in the vapor phase. As shown by *in situ* x-ray diffraction analysis, the hydration sequence continued normally until the assemblage C_3AH_6 + AH was obtained at 210°C and 2 mPa. These conditions were maintained for 72 hours, after which it was observed that the calcium aluminate-steam reaction had been suppressed. Examination of the test bar showed the presence of a reaction rim ∿0.7mm thick, composed mainly of C_2AS, β-CS, CA_2, and α-Al_2O_3. The silica had been dissolved from the cement by the steam and then transported to the surface of the test bar where it quickly reacted, forming calcium silicates and calcium aluminum silicates. Since silica impurities in coal would be expected to contribute dissolved silica to the pressurized steam of a gasification reactor, similar reactions between dissolved silica and an initially high purity calcium aluminate castable can be expected to occur.

The early stages of the hydration of specimen #3 of high alumina neat cement are shown in Fig. 1 to demonstrate the use of difference plots in the interpretation of patterns. Pattern No. 11 at the top of the figure was recorded at 207°C and 1.5 mPa after gradually increasing the temperature over a 24 hour period. Pattern No. 2 was recorded at room temperature. In the difference plot, the negative peaks all correspond to CA_2, meaning that this is the phase being consumed. The positive peaks correspond to AH and C_3AH_6, the products of the reaction. Difference plots have been prepared for several critical temperature ranges. They are particularly useful in showing which phases are involved in reactions and in distinguishing the reaction products from the phase or phases being consumed.

Plans: Data obtained from the high purity neat cement now being heated in steam will be analyzed, after which the same material will be tested in more complex atmospheres. A lime-alumina-silica refractory will also be examined by *in situ* x-ray diffraction, first in a steam atmosphere and then in a simulated gasification environment.

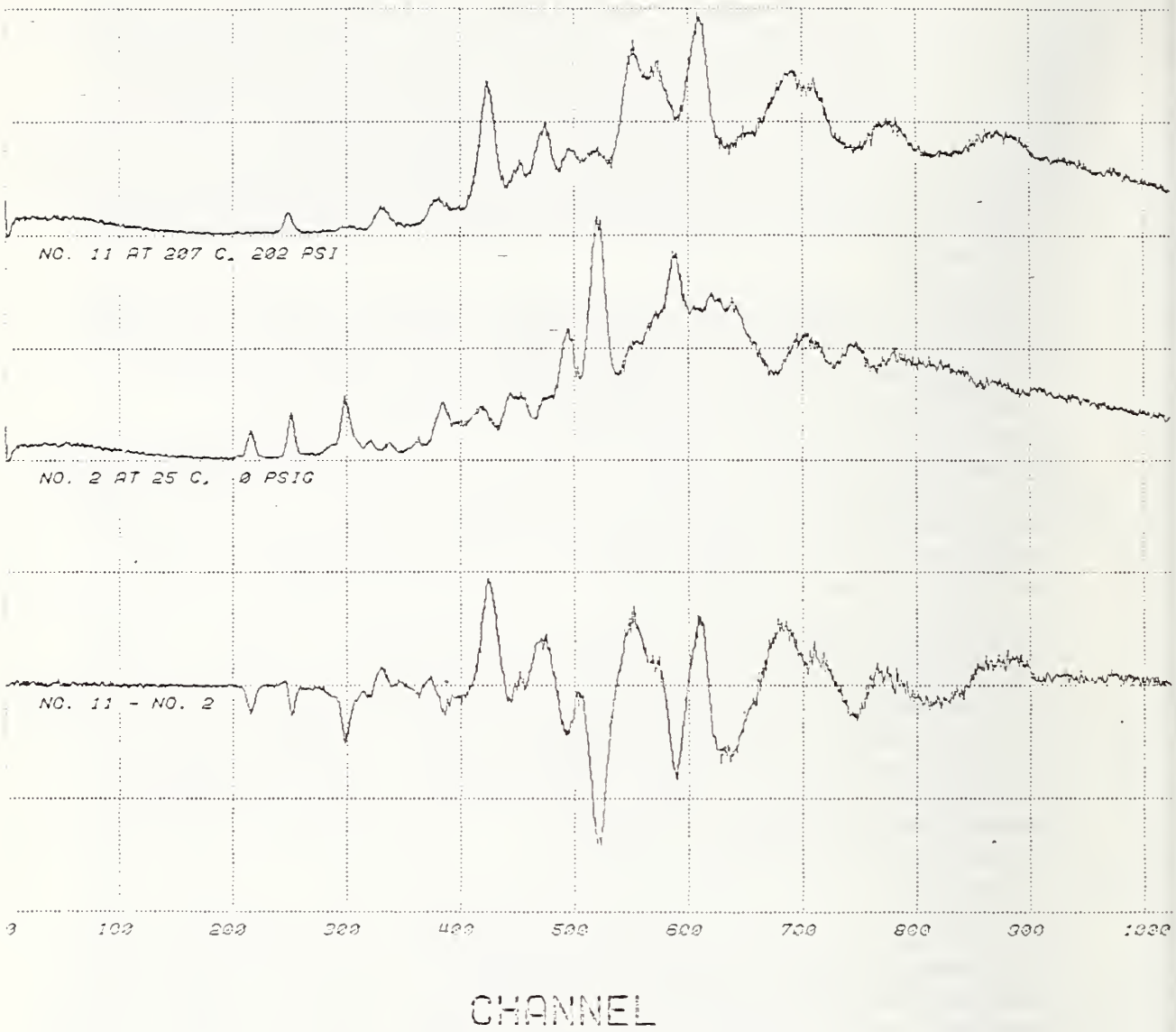

Figure 1. EDXD patterns for specimen #3 of high alumina neat cement heated in steam. The difference pattern formed by subtracting No. 2 from No. 11 shows the loss of CA_2 (negative peaks) on reaction with steam to form AH and C_3AH_6 (positive peaks).

TABLE 1. *IN SITU* X-RAY ANALYSIS OF HIGH ALUMINA NEAT CEMENT SPECIMEN #2 IN STEAM

Temperature (°C)	Pressure (psig)*	Time (hr)	X-ray Analysis and Remarks
25	0		CA_2, small amounts α-Al_2O_3, CA
93	~10	20	CA_2 major phase but intensities greatly reduced, C_3AH_6 and AH_3 present as minor phases
110	~15	46	C_3AH_6, AH_3, AH, α-Al_2O_3, trace CA_2
210	200	4	C_3AH_6, AH major phases, trace α-Al_2O_3
210	150	3	C_3AH_6, AH. Crystallinity of AH improving
210	150	15	C_3AH_6, AH. Well crystallized
210	150	7	C_3AH_6, AH, major phases, α-Al_2O_3 minor phase
100	15	3	C_3AH_6, AH, major phases, α-Al_2O_3 minor phase
365	1100	15	$C_4A_3H_3$, AH, major phases, α-Al_2O_3 minor phase
310	970	6	$C_4A_3H_3$, AH major phases, α-Al_2O_3 minor phase
410	1130	2	$C_4A_3H_3$, AH major phases, α-Al_2O_3 minor phase
410	1120	14	$C_4A_3H_2$, α-Al_2O_3, AH major phases. AH dissociating
410	1120	8	$C_4A_3H_3$, α-Al_2O_3, AH major phases. AH dissociating, α-Al_2O_3 forming
450	1130	1	ditto
450	1130	1	ditto
450	1130	1	ditto
475	1130	1	CA_2, CA, $C_4A_3H_3$, α-Al_2O_3 major phases, trace of AH
475	1130	15	CA_2, CA, $C_4A_3H_3$, α-Al_2O_3 major phases. CA_2 increasing
500	1075	3	CA_2, CA, $C_4A_3H_3$, α-Al_2O_3 major phases. CA_2 increasing
550	1100	4	CA_2, CA, α-Al_2O_3 major phases. CA_2 increasing
575	1100	22	CA_2, CA, α-Al_2O_3 major phases
600	1030	1	CA_2, CA, α-Al_2O_3 major phases. CA_2 increasing at the expense of Al_2O_3, CA
600	1030	3	ditto
600	1050	15	CA_2 major phase, α-Al_2O_3 minor phase
700	1000	3	ditto
800	1000	16	CA_2, trace α-Al_2O_3
900	1060	1	ditto
1000	1000	1	ditto

*in SI units - 1 mPa ≈145 psia

b. Slag Characterization (W. S. Brower, J. L. Waring, D. H. Blackburn and C. A. Harding, 565)

Progress: The high pressure viscometer is currently operational. In the present design the temperature of the rotating crucible (Figure 1, letter I) cannot be measured directly. Therefore a calibration between the melt crucible and the platinum heater (Figure 1, letter F) temperature must be established. This calibration is performed by inserting a thermocouple into the molten slag and measuring the temperature; concurrently, a separate thermocouple welded on the platinum heater is monitored. The results of the calibration are given in Figure 2. As might be expected, a linear relationship exists between the temperature of the crucible and tl temperature of the platinum heater at various pressures.

An iron silicate slag with low melting characteristics was selected for initial viscosity measurements. The composition is as follows: SiO_2 42 wt%, Al_2O_3 3 wt%, Fe_2O_3 25 Wt%, CaO 5 wt%, MgO 5 wt%, Na_2O 15 wt%, K_2O 5 wt%. Other iron silicates might be expected to exhibit similar behavior in steam pressures.

The results of the preliminary viscosity measurements are given in Figure 3. In the figure, $\log_{10} \eta$ (viscosity in poises) is plotted against temperature in degrees C. Curve A represents the viscosity at various temperatures and ambient pressure. Similarily curves B, C, D represent viscosity as a function of temperature at pressures of 60 psi, 80 psi and 95 psi steam respectively.*

The glass which was heated previously in steam (Fig. 3, curve C) was reheated at ambient pressure to outgas the included water vapor, then the viscosity was remeasured at ambient pressure. These results are shown in Figure 4; it can be seen that the viscosity has only increased slightly. The increase may be due to loss of alkali because of added and prolonged heat treatment or it may have been associated with the steam treatment. The composition was unusually high in Na_2O, loss of which would be expected to raise the viscosity. Loss of K_2O, would have the opposite effect but its volatility is less as well as its concentratio

Samples were taken from two slags which were quenched in air and steam respectively, to form glass and these were reheated at atmospheric pressur in air and the weight loss determined. The slag which had never been subjected to a steam atmosphere showed a weight loss of 0.03% at 1200 °C after 18 hours. A sample of the same slag subjected to 80 psi steam pressure at 1175 °C for about four hours, and quenched, showed a weight loss of 0.62% for the same conditions. Under these conditions, the slag did not achieve a constant weight, indicating further weight losses would be observed if held at temperature or longer time.

---

*In SI Units $p(\text{MPa}) = \frac{p(\text{psig}) = 14.7}{145}$

It can be noted from Figure 3, that the viscosity of this silicate melt appears to increase significantly with increasing steam pressure at constant temperature. This result is so unexpected that before these data can be completely believed, the experiment must be repeated. Figure 4 illustrates that no appreciable composition deviation has taken place in the slag. These experiments will be re-run in an attempt to determine whether or not the present data are valid.

After the last run at 95 psi, the pressure vessel was opened and inspected. The stainless steel interior was found to be slightly corroded and the refractory bricks surrounding the platinum heater were severely attacked. In addition, dendrites which appeared to be metallic copper had grown from the electrodes; water used to generate the steam in the bottom of the vessel was found to have a pH of about 3.2.

Plans: Several important modifications are currently being worked on to improve the capabilities of this apparatus. A new shaft is being prepared to hold the rotating crucible. This will be hollow so that a permanent thermocouple can be inserted to measure the crucible temperature directly. Other modifications will be made in the insulation and radiant heat reflector design in an attempt to cut down the large heat losses, which at the present, limit the temperature capability.

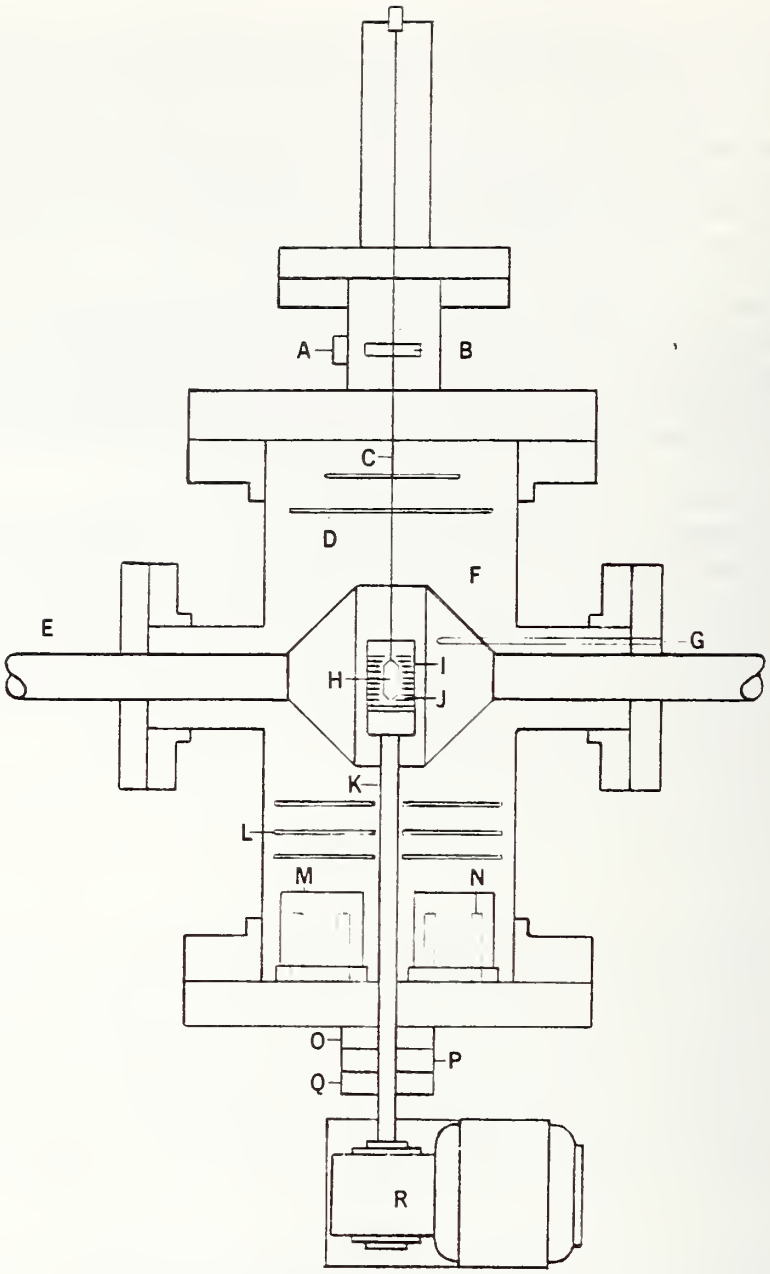

Figure 1. Full assembly schematic drawing of high pressure-temperature viscometer.

A - position detector
B - magnet
C - torsion wire
D - water condensation shields
E - electrodes
F - heating elements
G - temperature control thermocouple
H - bob
I - crucible
J - molten slag
K - spindle
L - anti-convection baffle
M - heat exchangers
N - bayonet heaters
O - shaft seal
P - shaft cooling jacket
Q - shaft bearing
R - shaft drive mechanism

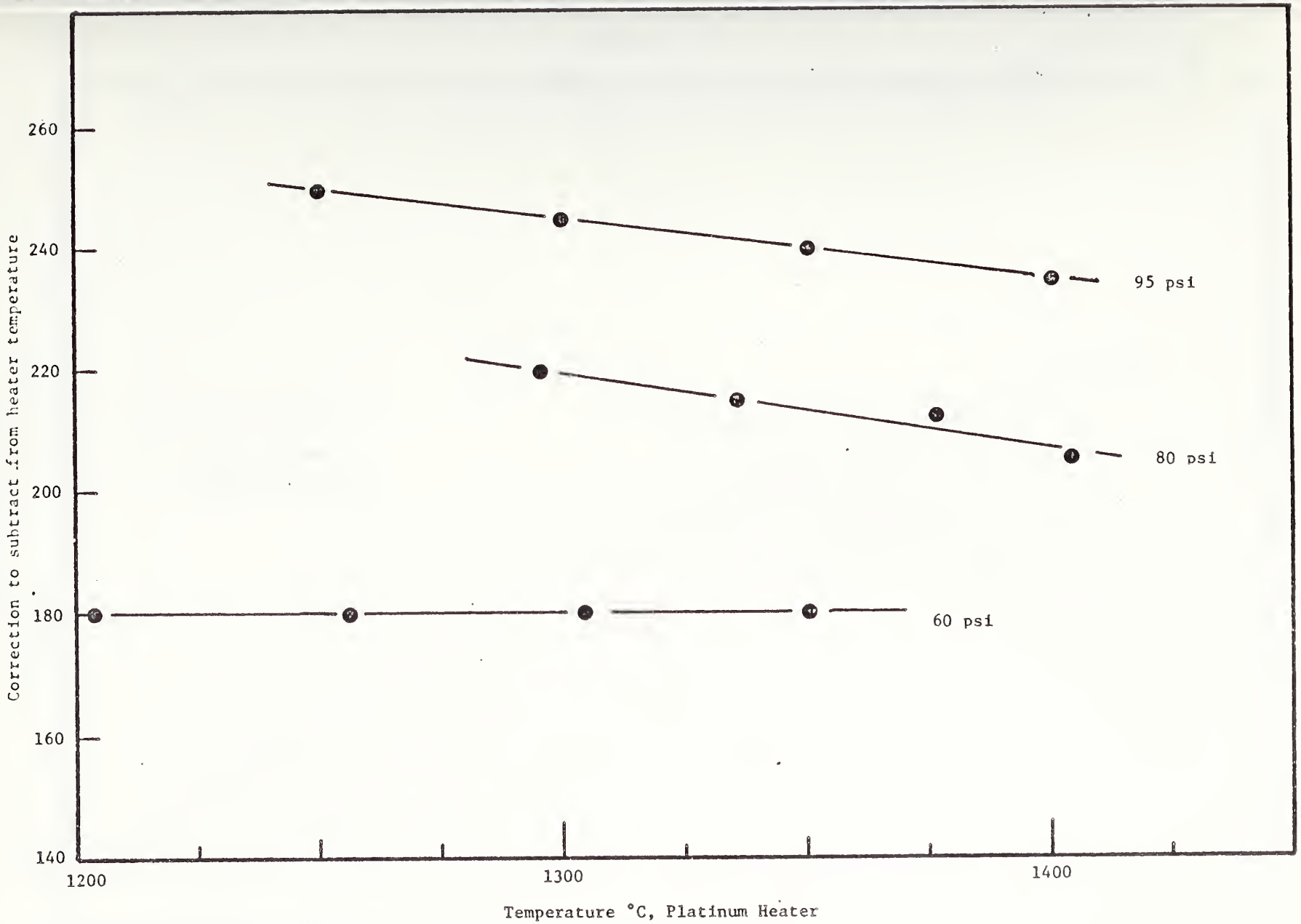

Figure 2. Calibration of heater temperature vs melt temperature.

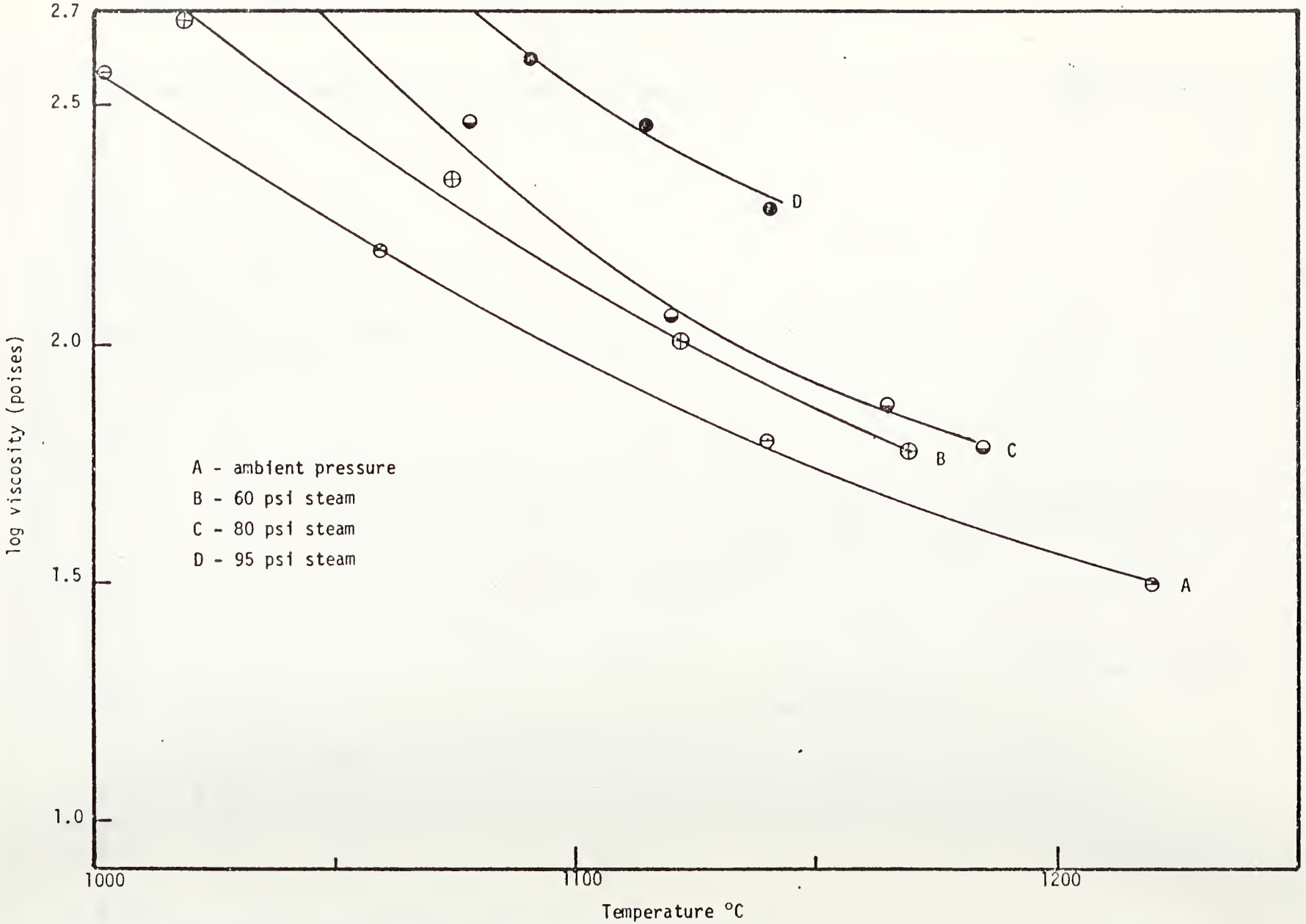

Figure 3. Log viscosity vs temperature for slag.

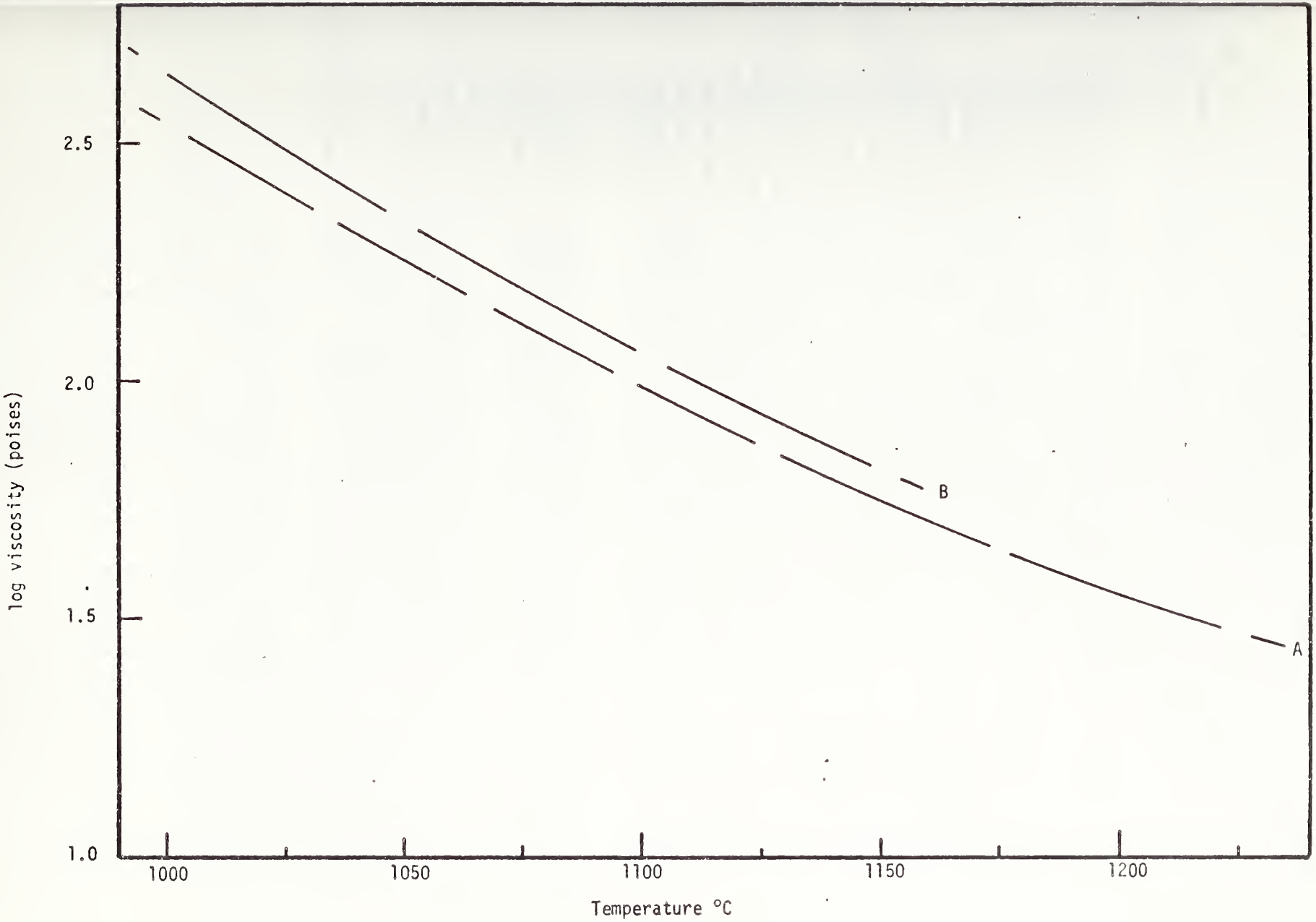

Figure 4. Viscosity of slag prior to steam treatment (A) and after exposure to 80 psi steam (B).

c. Vaporization and Chemical Transport (J. Hastie and D. Bonnell, 561)

Progress: *Probe Development.* The source of the problem of low beam intensities encountered with the reactor-mass spectrometer system during the previous quarterly reporting period has been identified. We have established that the reactor alignment is satisfactory but the beam is scattered by gas effusing through a micro crack in the reactor nozzle. This crack apparently developed as the result of chemical corrosion and we have modified the reactor design to reduce this effect.

Two new reactor sampling nozzle designs have been developed, the first having basically the same conical geometry as the original but with thicker walls to increase resistance to corrosion. The second nozzle utilizes a capillary tube rather than a thin walled cone as the gas probe. The major fundamental difference between these two types of sampling nozzle is that the capillary probe allows sample wall-gas collisions to occur as the gas passes through the sampler from the high-pressure reaction zone to the low pressure region of the mass spectrometer system. However, this effect has the advantage of reducing the rate of gas flow into the vacuum chamber and thereby allowing higher reactor pressures to be utilized by a factor of about two. The constructed capillary is essentially a 1.9 cm long thick-wall platinum tube with an average inner diameter of about .01 cm. This probe has been tested, as described below, in an alkali silicate corrosive slag-like atmosphere without incurring problems such as orifice plugging or enlargement due to corrosion. Thus for corrosive samples, this type of probe should be more satisfactory than the prototype thin wall nozzle design used previously. However, we should stress that such a probe should only be used for equilibrium systems since the wall collisions would disturb the composition of a kinetically controlled system. The less robust conical-type sampling nozzle will be used for non-equilibrium systems if necessary.

Reactor Equilibrium and Sampling Fidelity. As we have stressed in previous reports, it is important to determine the range of pressure, composition and temperature conditions for which the reactor attains an equilibrium condition and for which the sampling process does not perturb the equilibrium. We have previously shown, using the Na_2SO_4 and NaCl test cases, that the vaporization processes have the expected enthalpy changes for an equilibrium process over a wide temperature interval. What remained to be established was the effect of reactant partial pressure on the apparent equilibrium constant, if any. The calibration salt Na_2SO_4 was used for this test. By adding an external source of SO_2 to the N_2 carrier gas we were able to test the reversibility of the process:

$$Na_2SO_4(\ell) = 2Na + O_2 + SO_2 \quad (K_p = pNa^2 \cdot pO_2 \cdot pSO_2)$$

under isothermal conditions at temperatures of around 1200 °C and total pressures in the region of 0.5 - 0.7 atm. The apparent equilibrium constant K_p, for this process was observed to be pressure independent,

as expected for a non-perturbed equilibrium process, for SO_2 partial pressures in the range of 10^{-4} - 10^{-2} atm, as shown in Figure 1. The average value of K_p over the pressure independent interval was found to be in good agreement with the expected literature value, as indicated in Figure 1. However, at both lower and high SO_2 pressures K_p varied. We believe that for relatively high pressures of reactant gas (SO_2 in this case), some of the gas passes through the reactor into the mass spectrometer system without having contacted the sample. Hence, the observed SO_2 signal would be higher than the equilibrium level and correspondingly so would K_p. Based on these observations, we have decided to introduce baffles into the reactor to increase the number of gas-sample collisions prior to sampling. This should increase the range of reactant pressures where equilibrium can be established.

Alkali Silicate Vaporization. High pressure (0.7 atm N_2) mass spectrometric analyses of the vapors over an alkali silicate oxide mixture of composition: SiO_2 (75 wt %), Na_2O (15.6), CaO (10) and SO_2 (0.4), plus minor amounts of HCl, H_2O and hydrocarbon impurities were made using the newly developed capillary probe. Nitrogen was used as the high pressure transport gas. Vapor species were observed over the temperature interval 1100 - 1250 °C and typical mass spectral data are shown in Figure 2. Not all the observed mass spectral ions were attributable to known molecular species. The identifiable molecular precursors of interest included Na, SO_2, HCl, O_2 and H_2O. Some of the unassigned peaks may be new Na-containing species whose identity can only be speculated on pending further study where the reactive gas pressures are varied isothermally. The observed HCl and H_2O components were formed from impurities contained in the oxide sample. Under the present conditions, the partial pressure of Na-containing species is of the order of 10^{-6} atm which is sufficient to result in transport and deposition of corrosive alkali deposits under expected coal gasification conditions. It will be of interest to determine in future planned studies the effect of reactive coal-gas atmospheric components on this alkali transport. However, the complexity of the observed mass spectra for this relatively simple system and the number of unassignable ion peaks reinforce our original expectation about proceeding with simple systems of gradually increasing complexity prior to analyzing actual coal slag-coal gas systems.

Thermodynamic Modeling of Slag-Coal Gas Interaction. During the past Quarter we initiated the modeling phase of our program. As was indicated in the original project proposal, sophisticated computer based modeling will be used to provide the necessary link between laboratory results and actual coal gasifier field data. A valid model should allow us to extrapolate the laboratory results of coal gas-slag-ceramic vapor transport obtained at relatively low pressures of about 1 atm to actual gasifier conditions of typically 20 atm. In the near term the modeling will be limited to equilibrium systems and will be used primarily as a guide to

the selection and interpretation of experimental systems. Essentially this phase of the modeling utilizes a computer program based on the so-called NASA Gordon and McBride code with the JANAF Thermochemical Tables as a data base. This particular program has been used previously in our laboratory for related combustion problems and can handle complex multi-component systems including both condensed and vapor phase species.

Essentially the computer program contains the basic thermodynamic data for many but not all of the gaseous vapor and condensed phase components pertinent to slag-ceramic-coal gas equilibria. For any specified set of reactants and conditions of temperature and pressure one can calculate the equilibrium composition. Typical output data for a representative slag-coal gas system are shown in Table 1. These data indicate a significant transport of alkali metal species and measurable amounts of iron (as $Fe(OH)_2$) and hydrogen cyanide to the vapor phase. We expect to compare future calculations of this type with our experimental data, such as those given in Figure 2. New vapor species observed experimentally will subsequently be included in the thermodynamic data base for the equilibrium program. However, the basic thermodynamic data for such species will first need to be determined either by auxiliary experiments, e.g., by Knudsen effusion studies of appropriate equilibria, or by estimation.

Plans: Pump failure due to the corrosive gases used in recent experiments will require a major overhaul, including upgrading the rubber seals, of the Roots blower used to back the main diffusion pump for the vacuum system.

The new capillary probe which appears quite satisfactory for slag sampling will be tested for its sampling fidelity by carrying out pressure independent studies using the Na_2SO_4 calibrant system.

The slag vaporization studies will be extended to reactive atmospheres containing, initially, H_2O and H_2. The effects of known partial pressures of H_2O and H_2 (in a N_2 atmosphere) on the mass spectra, and particularly the alkali metal and "unidentified" peaks, will be noted. By systematically varying the conditions of temperature and reactant partial pressure we should be able to identify the previously unidentifiable mass spectral ions and determine their possible significance to vapor transport. Any departure from thermodynamic equilibrium should also be apparent from such data.

Complementary modeling calculations will be made for the experimental systems using the JANAF data base.

Table 1

Thermodynamic[a] Prediction of Vapor Transport at 1300K and 23.8 atm

Major gases		Condensed Mineral Matter[b]		Inorganic Vapor Species	
CH_4	1.0(-3)[c]	Al_2O_3	1.8(-3)	NaOH	3.4(-4)
CO	2.0(-1)	FeO	7.1(-3)	Na	5.3(-5)
COS	2.7(-4)	NaOH(1)	4.9(-3)	$Fe(OH)_2$	5.2(-7)
CO_2	1.0(-1)	SiO_2	1.8(-3)	HCN	3.7(-7)
H_2	3.3(-1)			SiO	8.6(-14)
H_2O	3.2(-1)				
H_2S	1.4(-2)				
NH_3	3.9(-5)				
N_2	4.4(-3)				

(a) 1971 edition of JANAF Thermochemical Tables used as data base.

(b) Condensed components assumed to have unit thermodynamic activity.

(c) 1.8(-3) denotes mole fraction 1.8×10^{-3}.

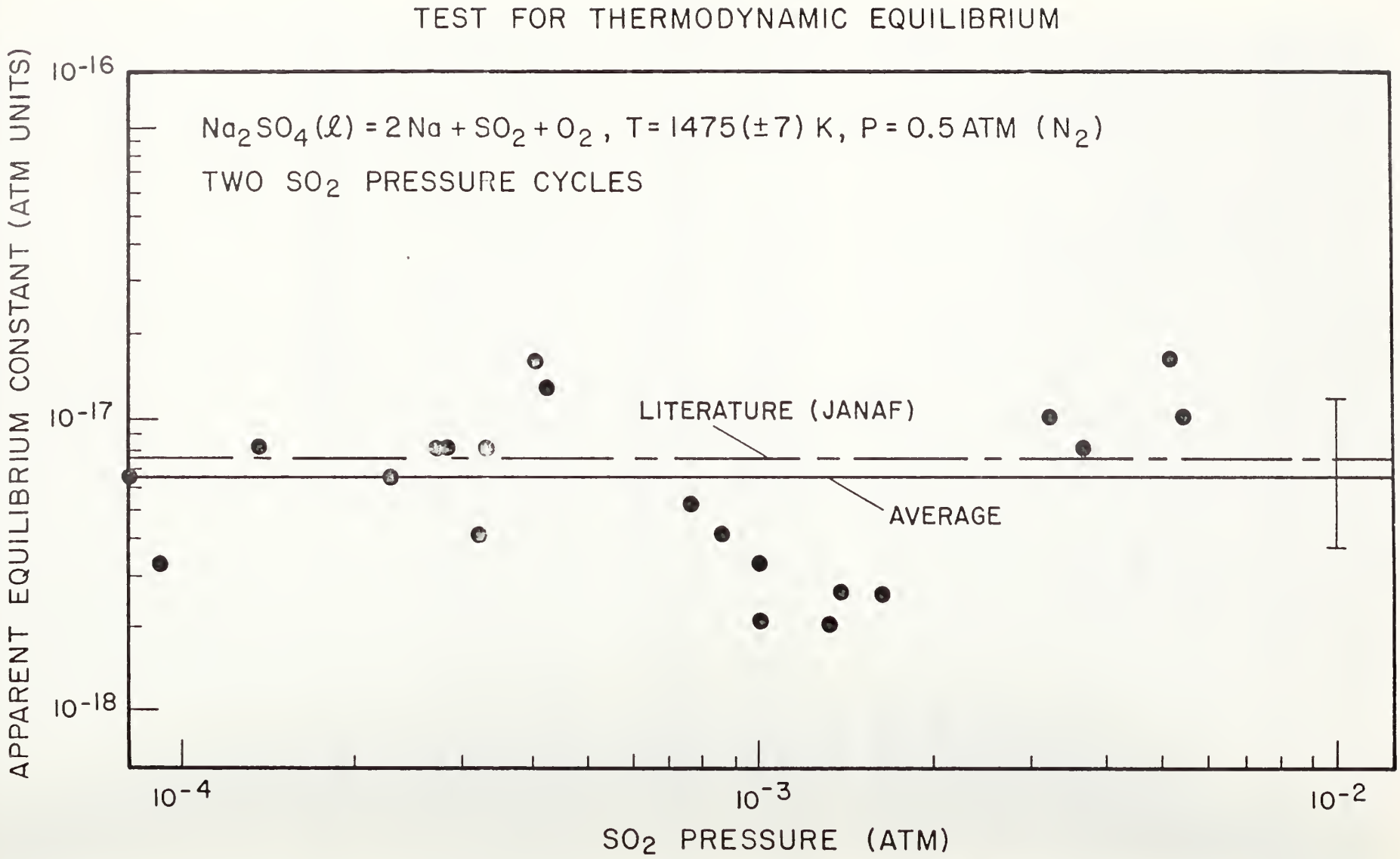

Figure 1. Plot demonstrating the presence of equilibrium for the Na_2SO_4 vaporization process in a N_2 atmosphere by virtue of the invariance of the equilibrium constant with partial pressure

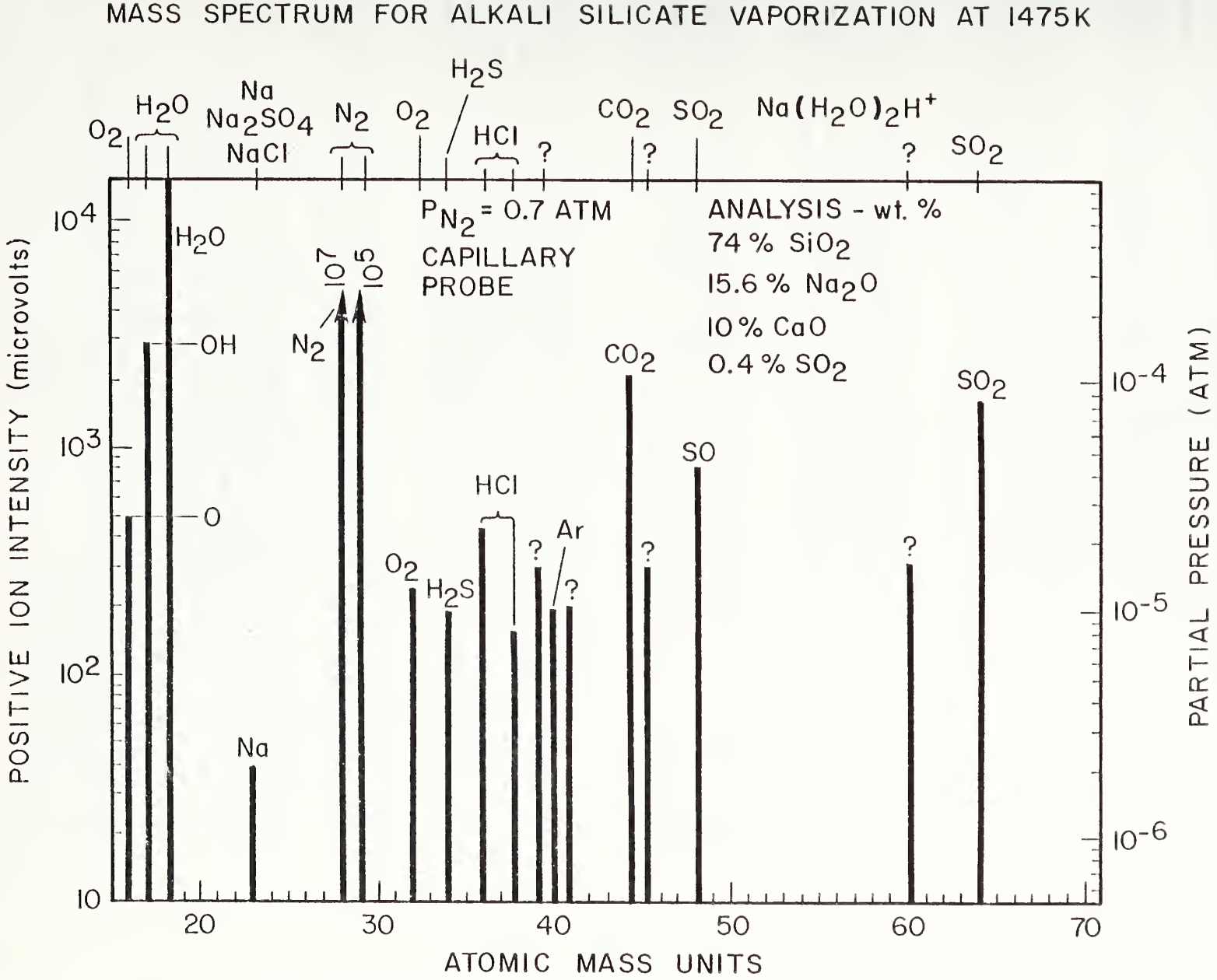

Figure 2. Typical mass spectrum for vaporization of the alkali silicate SiO_2 (74 wt %), Na_2O (15.6), CaO (10, SO_2 (0.4) in a N_2 atmosphere at 1475 K using an isothermal capillary probe.

4. Failure Prevention

a. Failure Information Center (R. C. Dobbyn, W. A. Willard and J. H. Smith, 562)

Progress: During the quarter the Failure Prevention Information Center received 37 reports of operational experiences and components and materials failures in coal conversion pilot plants and process development units. This number includes several diagnostic failure analyses from Argonne National Laboratories and Oak Ridge National Laboratories. To date, the percent contribution of information items received from different coal conversion processes is shown in Table 1.

These reports have been classified and evaluated for technical completeness and accuracy and discrepancies have been resolved. Detailed abstracts of this information have been entered into the Center's computerized data bank. A recent update of the frequency of failure modes, which analyzes all information in the system, is shown in Table 2.

The Information Center continued to aid Battelle-Columbus in their preparation of the DoE Materials and Components Newsletter feature on failure experiences. Weekly updates of all abstracts are furnished to Battelle together with complete hard copy of certain reports when requested During the quarter, the Center furnished 45 updated summaries and 18 complete reports.

The Information Center also handled 25 other requests for information during the quarter. In response to these inquiries, copies of 645 abstracts and several draft reports were transmitted. In addition, six visitors to the Center were briefed on its scope, operation and future plans.

During this quarter, major emphasis was placed on completing the analysis of the performance of materials and components used in the Conoco CO_2 Acceptor Process Pilot Plant during its five and one-half years of operation. Over 2400 operating events which resulted in process upsets or run terminations have been investigated and analyzed. A detailed report covering both metals and refractory materials is now in preparation and will be forthcoming during the next quarter.

Direct contact with operating pilot plants, process development units and failure analysis laboratories continued; the Synthane, Hygas and Westinghouse and BCR-Bigas plants continued to interact with the Center.

One presentation was made and one paper was published by J. H. Smith, describing failure experiences with Incoloy 800. Center staff also participated in the annual Metals Properties Council Subcommittee 9 devoted to the properties of materials for coal conversion.

Plans: Plans for the next quarter include completion of the final report covering the CO_2 Acceptor Process pilot plant and a similar, but less detailed, report covering the operating experiences to date at the IGT Hygas pilot plant.

In addition, liaison with the remaining gasification and liquefaction pilot plants and PDU's*--those not yet visited--will be stepped up. Our success with Synthane, Hygas, Bigas, etc., has demonstrated that this technique works.

The format of failure data entries is being revised to facilitate information exchange and further, in-depth analysis of common problems. These analysis will become the subject of future reports issued periodically and supplied to DoE for distribution. Submittal of candidate topics and report outlines for DoE concurrence is also planned during the next quarter.

---

*PDU = Process Demonstration Unit

Table 1

COAL CONVERSION PROCESSES

NO OF ITEMS	PERCENT	PROCESS
7	1.28	ALL
17	3.12	BIGAS
1	0.18	BIOMASS
38	6.98	BMI
10	1.83	CARBONATE
21	3.86	CLEAN COKE
1	0.18	COED
73	13.41	CO2
2	0.36	CPC
2	0.36	EXXON
3	0.55	GFERC
76	13.97	HYGAS
1	0.18	LERC
23	4.22	LIGNITE
20	3.67	MERC
34	6.25	MISC.
1	0.18	ORNL
3	0.55	PERC
1	0.18	RANN
2	0.36	SEVERAL
34	6.25	SRC
6	1.10	SRC-W
131	24.08	SYNTHANE
5	0.91	SYNTHOIL
1	0.18	UNKNOWN
31	5.69	WESTINGHOUSE

Table 2

NUMBER OF REPORTED INCIDENTS OF FAILURES
IN COAL CONVERSION PLANTS* **

FAILURE MODE ANALYSIS

PROCESS

FAILURE MODE	CO2	HYGAS	SRC	SYNTHANE	OTHER	TOTAL
CORROSION	48	37	11	29	67	192
AQUEOUS	0	2	0	0	3	5
CARBURIZATION	10	2	0	0	5	17
METAL DUSTING	4	0	0	0	3	7
OXIDATION	4	4	0	0	5	13
PITTING	3	7	3	7	9	29
SULFIDATION	16	12	0	8	5	41
GENERAL	11	10	8	14	37	80
STRESS-CORROSION	6	7	5	6	35	59
CHLORIDE	4	7	2	4	17	34
OTHER	2	0	3	2	18	25
MANUFACTURING DEFECT	14	10	13	25	47	109
DESIGN	6	4	13	15	33	71
FABRICATION	4	3	0	4	4	15
QUALITY CONTROL	4	3	0	6	10	23
EQUIPMENT MALFUNCTION	6	12	3	9	19	49
OVERHEAT	6	11	3	6	16	42
OVERSTRESS	0	1	0	3	3	7
EROSION	7	9	11	26	42	95
STRESS/TEMP FAILURE	1	6	1	7	16	31
CREEP	0	1	0	0	3	4
FATIGUE	0	2	0	4	10	16
THERMAL STRESS/SHOCK	1	3	1	3	3	11
UNKNOWN	4	11	0	27	17	59

* Incidents reported to NBS Failure Information Center - sponsored by DOE, Fossil Energy.

** Operating times and level of reporting vary with each plant.

INFORMATION SOURCE

R. C. Dobbyn

National Bureau of Standards

(301)921-2952

4. Failure Prevention

b. Materials Properties Data Center (H. M. Ondik and T. A. Hahn, 565 and I. J. Feinberg, 562

Progress: During the past quarter the detailed cataloguing of the contractors' reports has continued. The completed catalogue will make it possible to identify all reports covering information on a given property. The reports are being cross-checked with ORNL TIC and NTIS computer files to determine the availability of these reports for more general distribution. This information is also part of the catalogue. The NTIS and ORNL TIC bibliographic files will also provide other possible sources of pertinent data. A thesaurus (i.e., properties, materials) must be constructed in order to form a sound basis for computer filing and searching of the Materials Properties Data Base. The detailed cataloguing described above provides the initial entries for the thesaurus. The thesaurus will also have to provide other sets of words to permit flexible searching of the files, i.e., conditions of testing such as temperatures, pressures, chemical environments, etc. and also sets of keywords relating to the titles and general subjects of the projects.

The necessary equipment capabilities for the Data Center's computer-terminal facility have been fully defined and identified. The facility is to provide the following capabilities: text-editing of information before entering it into the main computer storage, cathode-ray tube display for checking before beginning printout operations, graphics editing and handling from digitizing of initial input to appropriate mechanisms for output. A properly designed equipment system can save a good deal in computer charges for central processing unit time, and in personnel time. Equipment components have been chosen and are on order for the establishment of the computer-terminal facility. The components we have chosen to buy initially can interact with NBS Computer Division graphics components, thereby providing us with some graphics capability until we can expand our facility to include our own graphics digitizer, plotter, and fast hard-copy printer. The equipment on order provides two terminals with appropriate linkages for cross-communication, as well as communication with the central computer. One terminal possesses a hard-copy printer, a dual-tape cartridge system, and sufficient self-contained buffer storage to permit complete proof-reading and text-editing of input material before entering data into the memory of the central computer. The second terminal, an "intelligent" one, has a cathode-ray tube display, a single-tape cartridge arrangement, a 2^{13} ($\sim$8000) byte (8 bit words per byte) core storage, and the appropriate capability and accompanying software for handling graphical material. Because of the core memory of the terminal, graphical information can be edited and corrected before entering into the central computer storage, as well as rearranged into graphical forms which may differ from the

original input in style, if that is desirable. Two modems, or couplers, are also on order which provide the link via telephone lines with the computer. The cost of the equipment components which are on order is being covered by NBS funds.

In order to assure that the best choice of computer Data Base Management System (DBMS) is made, the staff of the Center have arranged for and taken a brief course dealing with the subject, and have obtained expert advice. Investigation of DBMS availability has revealed two systems which present the best possibilities for the use of this Center. Both systems have several vendors and the details concerning each vendor facility capability with regard to each system, and the detailed properties of each DBMS must be carefully evaluated so as to choose the most advantageous combination, meaning usually the most flexible, economical, and reliable.

Three summary reports, covering three projects and some 20 contractors' reports are being prepared for DOE approval. They will cover, for a given project, work to date, or when possible, work done to a particular point in the research,providing a suitable summary of a given achievement or of a complete phase of the effort. The reports will be organized in sections which will be headed generally as follows: project title, investigators, objective(s), methodology, materials studied, properties investigated, experimental procedure, results (all to be presented as compactly as possible consistent with completeness). Some variation will, of course, occur due to the nature of a given project and the type of material found on the contractor's reports.

The principal investigator attended the MPC Subcommittee 9 meeting held in San Antonio during February; also, the meeting of consultants for the Coal Conversion Systems Technical Data Book in Chicago in March.

Plans: The regular operations of the Center will continue--cataloguing of report information, storage file design, preparation of data summaries, checking of the ORNL TIC and NTIS data bases. Choice of the Data Base Management System will be made. As the ordered equipment is delivered, the terminal facility wll be put in use and data will be entered into the system.